

AUTOMATIC LANDMARK GENERATION FOR NONLINEAR REGISTRATION OF ANATOMICAL AND FUNCTIONAL BRAIN MRI

Ladan Amini¹, Hamid Soltanian-Zadeh^{1,2,3,*}, Emad Fatemi-Zadeh⁴, Gholam Ali Hossein-Zadeh^{1,3}

¹Control and Intelligent Processing Center of Excellence, School of Electrical and Computer Engineering, University of Tehran, Tehran, Iran

²Department of Diagnostic Radiology, Henry Ford Health System, Detroit, Michigan, USA

³School of Cognitive Sciences, Institute for Studies in Theoretical Physics and Mathematics, Tehran, Iran

⁴School of Electrical Engineering, Sharif University of Technology, Tehran, Iran
e-mail: hamids@rad.hfh.edu

Abstract—A limitation of using linear registration methods for mapping functional magnetic resonance imaging (fMRI) data to anatomical MRI, required for both multi-subject analysis and visualization of brain activations, is its inability to correct the geometric distortion induced by field inhomogeneity. Consequently, linear methods such as MI (mutual information) do not accurately align fMRI and MRI. Nonlinear methods such as TPS (Thin Plate Spline) may do the job but they require manual identification of landmarks. Due to low speed, high cost, and user-dependency of manual landmark identification, a new algorithm for automatic landmark generation is presented in this paper. The nonlinear registration method along with new automatic algorithm is applied on real anatomical and fMRI data and the results are evaluated. Experimental results illustrate the method and its excellent performance.

Keywords - Automatic landmark generation, fMRI and MRI registration

I. INTRODUCTION

An essential preprocessing step for various applications in medical image analysis and display is registration of functional and anatomical images. The goal of this procedure is to obtain a transformation that aligns low resolution EPI (Echo Planar Imaging) images of the functional study onto the high-resolution anatomical images. Moreover, in multi-subject analysis of fMRI data, the EPI images of various subjects are registered to a unit (standard) atlas, to map functional activations onto the structural information visualized in the high-resolution anatomical images [1].

Functional and anatomical MRI registration is a challenging task [2]–[3]. Since fMRI datasets only have a few slices, interslice distance needs to be dealt with. In addition, local geometric distortions generated by gradient field nonlinearities and magnetic field inhomogeneities make registration of EPI images and spin echo images challenging. Due to these difficulties nonlinear registration methods are preferred. In nonlinear methods, landmarks selection is needed to solve the above fMR and MR registration problems. However, due to the low resolution of fMRI, it is difficult to locate anatomical structures and landmarks in the functional data. Hence, the task of automatic landmark generation is labor intensive.

There are approaches in this area that use a set of corresponding anatomical landmarks [1], [4]. Although some of the researchers proposed automatic detection of

landmarks [5]–[8], these techniques are not suitable for our application due to the low resolution and distortion of fMRI data. There are also some nonlinear methods that work without landmarks but they are computationally expensive.

In this article, the above problems are solved by defining robust landmarks using global features such as the principal axes of the brain and local features like curvature. Since manual generation of these landmarks demands human interaction, increases sensitivity, and affects the reproducibility of the method, a new fully automatic algorithm is presented to define the landmarks. The nonlinear thin plate spline (TPS) method with automatic landmark generation is applied on real anatomical and fMRI data and the results are compared to those of the MI method and a nonlinear method without landmarks by AIR (Automatic Image Registration) software [9]–[10] showing superiority of the proposed method.

II. METHODS

We used wavelet analysis proposed by Ruttiman, et al [11] to detect activated regions from fMRI data. To map the activation results onto the corresponding high resolution anatomical MR images, linear or nonlinear registration methods may be applied. Although nonlinear methods align them accurately, many of these methods need manual identification of landmarks by the user, which is time consuming and irreproducible. To avoid this limitation, we present a new algorithm to generate landmarks automatically. In this section, linear (MI)¹ and nonlinear (TPS)² methods are described briefly. Then, the new algorithm is explained.

A. Linear Registration Method

A well-known conventional linear method is based on mutual information (MI) [12]. In this method, the two image volumes that are to be registered are referred as the source volume (MRI) and the destination volume (fMRI). A voxel of the destination and source volume are denoted $u(x)$ and $v(x)$, respectively, where x represents the coordinates of the voxel.

¹ - Mutual Information (MI)

² - Thin Plate Spline (TPS)

Given that T is a transformation from the coordinate frame of the destination volume to the source volume, $v(T(x))$ is the source volume voxel associated with destination volume voxel $u(x)$. Note that in order to simplify some of the subsequent equations T is used both to denote the transformation and its parameterization. An estimate of the transformation is searched that registers the destination volume u and source volume v by maximizing their mutual information,

$$\hat{T} = \arg \max_T I(u(x), v(T(x))) \quad (1)$$

where x is treated as a random variable over coordinate locations in the destination volume. Mutual information is defined in terms of entropy as [13]:

$$I(u(x); v(T(x))) \equiv h(u(x)) + h(v(T(x))) - h(u(x); v(T(x))) \quad (2)$$

where $h(\cdot)$ is the entropy of a random variable and is defined as $h(x) \equiv \int -p(x) \ln p(x) dx$, while the joint entropy of two random variables x and y is:

$$h(x; y) \equiv \int -p(x; y) \ln p(x; y) dx dy \quad (3)$$

B. Nonlinear Registration Method

The nonlinear TPS method [14] considers a radial basis function (RBF) ($r^2 \log(r^2)$) and an affine term. The affine coefficients have stronger effect when there is no need for nonlinear registration. The nomination of TPS is because of optimizing the bending energy of a thin plate subjected to only slight bending.

$$\min_{\psi} \left\{ \sum_{k=1}^D J(\psi_k(\underline{x})) \right\} \quad (4)$$

where ψ is the RBF function and the bending energy, J , is:

$$J(f) = \|f(\underline{x})\|^2 = \int_{R^2} \left(\frac{\partial^2 f}{\partial x^2} + 2 \frac{\partial^2 f}{\partial x \partial y} + \frac{\partial^2 f}{\partial y^2} \right)^2 dx dy \quad (5)$$

A unique solution based on previous criteria is based on $r^2 \log(r^2)$. The formulation is as below.

$$g(r) = -r^2 \log(r^2) \quad (6)$$

$$x_k^{new} = a_{o0} + a_{o1} x_k^{old} + a_{o2} y_k^{old} + \sum_{i=1}^N \omega_{oi} g \left(\sqrt{|x_k^{old} - x_i|^2 + |y_k^{old} - y_i|^2} \right) \quad (7)$$

$$y_k^{new} = a_{i0} + a_{i1} x_k^{old} + a_{i2} y_k^{old} + \sum_{i=1}^N \omega_{i1} g \left(\sqrt{|x_k^{old} - x_i|^2 + |y_k^{old} - y_i|^2} \right) \quad (8)$$

where (x_k^{old}, y_k^{old}) and (x_k^{new}, y_k^{new}) are the coordinates of each pixel before and after registration, respectively, a and ω are coefficients of affine and nonlinear terms, respectively. The following constraints decrease the effect of nonlinear term when the transformation is not nonlinear.

$$\sum_{k=1}^N \omega_{ok} = \sum_{k=1}^N \omega_{1k} = 0 \quad (9)$$

$$\sum_{k=1}^N x_k \omega_{ok} = \sum_{k=1}^N y_k \omega_{1k} = 0 \quad (10)$$

$$\sum_{k=1}^N x_k \omega_{1k} = \sum_{k=1}^N y_k \omega_{ok} = 0 \quad (11)$$

The TPS method is landmark-based and due to the geometric distortion of fMRI, registration results may be very sensitive to landmarks positions. In the following section, we introduce most appropriate landmarks and a fully automatic algorithm to find them.

C. Automatic Landmark Generation (ALG)

We have developed the following algorithm to identify anatomical landmarks automatically.

1- The cortex boundary is extracted and the centroid of the area inside the boundary (ROI)¹ is obtained.

For boundary extraction of MRI, a smoothing filter is applied on the original image, a clustering method (fuzzy c-means) is utilized with fuzzification degree and number of clusters equal to 1.3 and 4, respectively (Fig. 1). The third cluster is selected. For skull removal, the negative of the first cluster is eroded and its zero value pixels are set zero in the third cluster. To remove the holes and fill the area inside, closure and filling (morphological operations) are applied, respectively. The result is labeled and the largest (area) cluster is chosen. Cortex boundary and the centroid of area inside (ROI) are obtained.

For boundary extraction of fMRI, a threshold equal to 0.2 is applied on the normalized image instead of applying FCM clustering. The remaining steps to obtain the contour are the same as MRI contour extraction.

2- Principal axes of ROI are calculated using the Hotelling transform [15]. Passing the two perpendicular eigenvectors through the centroid found in Step 1 gives the principal axes of ROI. Fig. 2.a. from left to right shows the principal axes of MR and fMR images, respectively.

3- The intersections of the principal axes and the cortex boundary found in Step 1 are obtained.

4- Four neighborhood curves around the coincident points are considered. Fig. 2.a from left to right shows these four curves by highlighting regions of cortex boundary for MR and fMR images, respectively.

5- The curvature of the boundary points are calculated [16]. Curvature (C_i) is determined at each point of the cortex boundary as the vector difference between the unit distance vectors ($d_i = \frac{\|D_i\|}{D_i}$, D_i : Distance vector) of two

joining edge segments,

$$C_i = d_i - d_{i-1}. \quad (12)$$

6- Around the intersection points on the fMRI and MRI, the cortex boundaries are searched to get the pair locations that have the most similar curvatures. The search is

¹- Region of Interest (ROI)

started from the intersection points. The first two locations from the cortex boundaries that have closest curvature values are selected as landmarks. Fig. 2.b from left to right shows selected landmarks for the MR and fMR images, respectively.

III. EXPERIMENTAL RESULTS

A. Data

A healthy volunteer was studied using a block design periodic fMRI paradigm in which the subject performed a sequential finger to thumb opposition task. A total of 112 volumes were acquired from the subject using the EPI pulse sequence. Each volume contained 20 axial slices of size 64×64 , and covered a $FOV = 250 \times 250 \times 100 \text{ mm}^3$ with no gaps between slices. The task paradigm included four cycles (of 84 seconds each) of self-paced sequential finger to thumb opposition. In addition to the EPI data, a high-resolution 3D anatomical T_1 -weighted image volume was scanned from the subject using a magnetization-prepared rapid acquisition gradient echo (MP-RAGE) sequence. The scan parameters for this sequence were $FOV = 256 \times 256 \times 190 \text{ mm}^3$, with a matrix size of $256 \times 256 \times 190$ voxels, yielding a 1 mm^3 isotropic voxel size. To get corresponding slices of MRI and fMRI, data is coregistered and resliced using the SPM software.

B. Evaluations

In this section, we demonstrate the performance of the registration approach using the above real data set. In the motor task of fMRI experiment, we expect the cerebellum and motor cortex to be activated. These regions are mainly located in slices 20 and 74.

Registration procedure starts with coregistering and reslicing of fMR and MR images. Then the new automatic landmark generation (ALG) algorithm is applied to find landmarks. An affine transformation is used to obtain the primary coefficients of the MI method. Finally MI and TPS methods are applied and activation results overlaid on the registered images. Figs. 3 shows registration results of TPS with ALG algorithm, MI and nonlinear without landmarks (AIR software) methods on slices 20 and 74. Fig. 3.a from left to right shows the MRI and fMRI with activation overlaid, respectively. Fig. 3.b from left to right shows registered images with MI and TPS (with ALG algorithm) methods, respectively, superimposed on the same fMRI outlines (cortex boundary). The mismatch of the MI method is apparent as expected due to the inability of linear registration methods in fMRI and MRI alignment (because of mentioned problems in Section I); the arrows point to the mismatches. Fig. 3.c from left to right shows activation results superimposed on the registered images with MI and TPS (with ALG algorithm) methods, respectively. Fig. 3.d shows the same results as part c for the nonlinear method without landmarks (AIR). Fig. 3.e-h shows the same results as parts a-d (slice 74) for slice 20. It is evident that the nonlinear registration (TPS method with ALG algorithm) is

superior to linear method at preserving edge voxels in the analysis. The nonlinear method without landmarks (AIR) is quantitatively compared with the other two methods in Table 1. The comparison is done by calculating the mutual information between the registered MR image and its corresponding fMR image in all three mentioned methods. The nonlinear method in AIR utilizes a polynomial with 12 parameters. Note that the nonlinear method (TPS) along with the proposed ALG algorithm has generated more accurate results compared to the linear method (MI) and nonlinear method without landmark (AIR).

IV. SUMMARY AND CONCLUSION

Since the fMR images are geometrically distorted, the spatial relationship between fMRI and MRI is nonlinear. Therefore, linear registration methods are not suitable for the mapping of fMRI activations onto MRI; nonlinear methods are more appropriate for this application.

Nonlinear registration methods are landmark-based or without landmark that are computationally expensive. The landmarks can be identified manually or automatically. Compared to manual landmark identification, automatic landmark identification has the advantages of higher speed, lower cost, and user-independency. We have developed an automatic landmark identification algorithm. Although this has been done for the registration of fMR and MR images, it is applicable to other applications such as image guided surgery and intervention and pre-surgery simulation (virtual reality environment).

We have compared three registration procedures (nonlinear (TPS) with ALG algorithm, nonlinear without landmark (AIR), and linear registration methods). The nonlinear (TPS) method with the proposed ALG algorithm is superior for our application and satisfies our goal of mapping brain activations extracted from fMRI data onto the MRI easily, accurately, reproducibly and automatically.

ACKNOWLEDGMENT

The authors would like to thank Mr. M. Solaymani at Univrsity of Tehran, Control and Intelligent Processing Center of Excellence for his valuable help with the software.

REFERENCES

- [1] M. Otte, "Elastic Registration of fMRI Data Using Bézier-Spline Transformations," *IEEE Trans. Med. imag.*, vol. 20, no. 20, pp. 193-206, 2001.
- [2] R. Shekhar, V. Walimbe, S. Raja, V. Zagrodsky, M. Knvinde, G. Wu, B. Bybel, "Automated 3-Dimensional Elastic Registration of Whole-Body PET and CT from Separate or Combined Scanners," *J Nucl Med.*; vol. 46, no. 9, pp. 1488-1496, 2005.
- [3] ZF. Knops, JB. Maintz, MA. Viergever, JP. Pluim, "Normalized Mutual Information Based Registration Using k-means Clustering and Shading Correction," *Med. Imag. Anal.*, vol. 16, 2005.

[4] A. Ghanei, H. Soltanian-Zadeh, M. A. Jacobs, and S. Patel, "Boundary-Based Warping of Brain MR Images," *Journal of Magnetic Resonance Imaging*, vol. 12, pp. 417-429, 2000.

[5] MY. Wang, CRJ. Maurer, JM. Fitzpatrick, et al. "Automatic Technique for Finding and Localizing Externally Attached Markers in CT and MR Volume Images of the Head," *IEEE Trans Biomed Eng*, vol.43, pp. 627-637, 1996.

[6] C. Drewniok, K. Rohr, "Model-based detection and localization of circular landmarks in aerial images," *Int J Comp Vision*, vol. 24, pp. 187-217, 1997.

[7] T.-S., Kim, M. Singh, W. Sungkarat, C. Zarow, H. Chui, "Automatic registration of postmortem brain slices to MRI reference volume," *IEEE Transactions on Nuclear Science*, vol. 47, pp. 1607-1613, Aug 2000

[8] A.D. Brett and C.J. Taylor, "A Framework for Automated Landmark Generation for Automated 3D Statistical Model Construction," *Book Information Processing in Medical Imaging: 16th International Conference, IPMI'99, Visegrád, Hungary*, vol. 1613, pp. 376-381, 1999.

[9] RP. Woods, ST. Grafton, JD. Watson, NL. Sicotte, JC. Mazziotta, "Automated image registration. II. Intersubject validation of linear and nonlinear models," *J Comput Assist Tomogr*, vol. 22, pp. 153-165, 1998.

[10] FA. Nielsen, MS. Christensen, KH. Madsen, TE. Lund, and L. Kaihansen, "fMRI Neuroinformatics," *IEEE Eng. In Medicine And Biology*, pp. 112-119, 2006.

[11] U. E. Ruttimann, M. Unser, R. R. Rawlings, D. Rio, N. F. Ramsey, V. S. Mattay, D. W. Hommer, J. A. Frank, and D. R. Weinberger, "Statistical Analysis of Functional MRI Data in the Wavelet Domain," *IEEE Trans. Med. Imag.*, vol. 17, no. 2, pp. 142-154, 1998

[12] W. M. Wells, P. Viola, H. Atsumi, S. Nakajima, "Multi-Modal Volume Registration by Maximization of Mutual Information," *Med. Imag. Anal.*, vol. 1, no. 1, pp. 35-51, 1996.

[13] A. Papoulis, *Probability, Random Variables, and Stochastic Processes*, McGraw-Hill, Inc., third edition, 1991.

[14] F.L. Bookstein, "Principal Warps: Thin-Plate Splines and the Decomposition of Deformations," *IEEE Trans. Pattern Analysis Machine Intelligence*, vol. 11, no. 6, 1989.

[15] R. C. Gonzalez and R. E. Woods, *Digital Image Processing*. Reading, MA: Addison-Wesley, 1992.

[16] L. Amini, H. Soltanian-Zadeh, C. Lucas, and M. Gity, "Automatic Segmentation of Thalamus From Brain MRI Integrating Fuzzy Clustering and Dynamic Contours," *IEEE Trans. Biomed. Eng.*, vol. 51, no. 5, pp. 800-811, 2004.

Table 1: Quantitative comparison of three registration methods, linear (MI), nonlinear (TPS) with ALG algorithm, and nonlinear without landmark (AIR software) by calculating the mutual information between the registered MR image and its corresponding fMR image.

Slice 74	Slice 20	MI
0.3724	0.3208	Linear Method
0.6040	0.6765	Nonlinear Method (TPS with ALG algorithm)
0.5414	0.5969	Nonlinear Method (AIR)

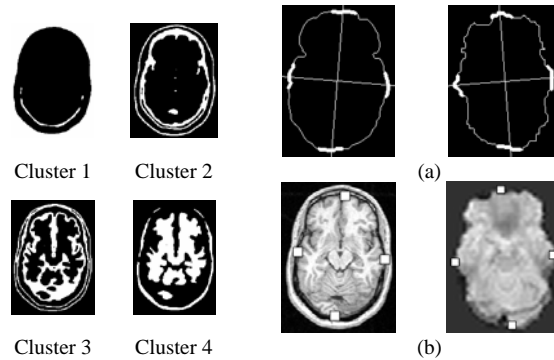


Fig. 1. Result of applying fuzzy c-means algorithm on the original MR image.

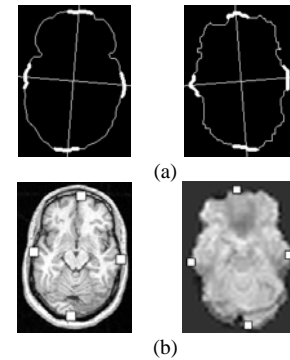


Fig. 2. From left to right, a) the principal axes and four neighborhood curves around the coincident points by highlighting regions of cortex boundary of MR and fMR images, respectively; b) selected landmarks by new ALG algorithm for MR and fMR images, respectively.

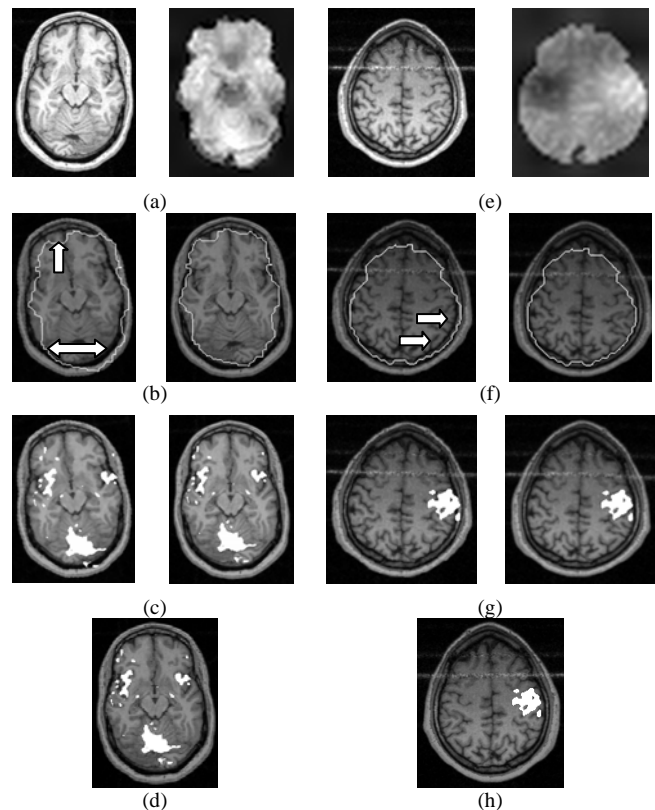


Fig. 3. From left to right, a) corresponding MR and fMR images of slice 74, respectively; b) contours of the registered fMRI using MI and TPS (with ALG algorithm) methods, respectively, superimposed on the MRI. The arrows point to the mismatch of the MI method; c) activation results superimposed on the registered MR images using MI and TPS (with ALG algorithm) methods, respectively. d) the same result as part © for nonlinear without landmarks method (AIR). (e)-(h) the results for slice 20. Note that with the MI registration, part of the activation region falls outside of the brain which is apparently incorrect. This is corrected by the TSP with ALG method.